PIBB 生物化学与生物物理进展
Progress in Biochemistry and Biophysics
2007, 34(3): 260~266
www.pibb.ac.cn

High-bone-turnover Osteoporosis and Aortic Calcification in *Opg* Knockout Mice*

XU Yong[1,2], YANG Hua[2], QIAO Jian-Ou[1,2], Li Xi-Hua[1,4], YAN Lan-Zhen[2], WANG Long[2,3], XU Guo-Jiang[2], FEI Jian[2], Fu Ji-Liang[2], WANG Zhu-Gang[1,2,3,4]**

([1]*Department of Medical Genetics, Shanghai Jiao Tong University Medical School, Shanghai* 200025, China; [2]*Shanghai Research Center for Model Organisms, Shanghai* 201203, China; [3]*State Key Laboratory of Medical Genomics, Rui-Jin Hospital affiliated to Shanghai Jiao Tong University Medical School, Shanghai* 200025, China; [4]*Laboratory of Genetic Engineering, Institute of Health Sciences Jointly Funded by Shanghai Jiao Tong University Medical School and Shanghai Institutes for Biological Sciences of The Chinese Academy of Sciences, Shanghai* 200025, China)

Abstract Bone turnover is regulated by local concentrations of cytokines such as osteoprotegerin (OPG) and receptor activator of nuclear factor kappaB ligand (RANKL). To explore the *in vivo* biological function of *Opg* and the mechanism of osteoporosis due to deficiency of *Opg*, *Opg* knockout mice have been generated through homologous recombination. $Opg^{-/-}$ mice exhibit a sharply decrease in bone density and strength as expected. The number of osteoclasts in $Opg^{-/-}$ mice significantly increases. Morphologically, osteoclasts appear more cuboidal in shape in $Opg^{-/-}$ mice than those of *wt* mice, suggesting that active osteoclastogenesis occurs in the absence of *Opg*. In consistent with this finding, an increase of osteoblast activity was also observed with accelerated mineral accumulation rate by histomorphometric measurement and elevated serum alkaline phosphatase activity (ALP) in $Opg^{-/-}$ mice. Interestingly, more than 50% of 2-month-old $Opg^{-/-}$ mice manifest medial calcification of aorta with comparable serum concentrations of calcium and phosphorus to *wt* mice. In conclusion, $Opg^{-/-}$ mice have a high-bone-turnover type osteoporosis. The aortic calcification in $Opg^{-/-}$ mice is not due to abnormality of calcium and phosphorus metabolism. The mechanism underlying aortic calcification in $Opg^{-/-}$ mice needs to be further investigated.

Key words *Opg* knockout mice, osteoporosis, aortic calcification, bone turnover, calcium and phosphorus metabolism

Osteoporosis is a skeletal disorder characterized by low bone density and compromised bone strength predisposing to an increased risk of fracture. Consequences of osteoporosis can be serious. An average of 24% of hip fracture in patients aged 50 years and over die in the year after fracture [1]. Nowadays it has become one of major public health concerns with its increasing prevalence. Arterial calcification is ectopic mineral deposition. It occurs with advancing age, often leads to serious clinical consequences (such as myocardial infarction, stroke and sudden death) [2]. Arterial calcification and osteoporosis frequently occur together and share many of the same risk factors. A recent clinical study even found that a significant age-independent association between the degree of aortic calcification and bone density, and a strong inverse relation between gains in vascular calcification and bone loss [3]. However, the common mediators of vascular and bone cell biology have long remained elusive.

Osteoprotegerin (OPG) is a glycoprotein as a soluble member of the tumor necrosis factor receptor superfamily. *Opg* deficient mice have shown severe osteoporosis and early onset arterial calcification [4]. RANKL is a membrane-bound protein of the tumor necrosis factor ligand family that is expressed on the osteoblast cell surface and has been shown to play a major role in osteoclast differentiation along with macrophage colony stimulating factor. RANKL binds to its receptor RANK on hematopoietic cells and initiates a cascade of signaling events that leads to

*This work was supported by grants from The Hi-Tech Research and Development Program of China (2001AA216081, 2004AA216081), The National Natural Science Foundation of China for Outstanding Young Scientists (39925023), Ministry of Education (00TPJS111) of China, Science and Technology Commission (99JC14029, 99XD14005), E-Institutes of Shanghai Municipal Education Commission (E03003).
**Corresponding author .
Tel/Fax: 86-21-64457997, E-mail: zhugangw@shsmu.edu.cn
Received: August 11, 2006 Accepted: December 13, 2006

osteoclast differentiation. As a decoy receptor for RANKL, OPG can prevent its interaction with the cognate receptor RANK. It has been shown to be a potent inhibitor of bone resorption through interfering osteoclast survival, differentiation and biological activity *in vitro* [5]. Therefore the unbalance of OPG/RANKL can lead to bone loss in *Opg* deficient mice. But the molecular mechanism of *Opg* in the progress of vascular calcification is still unclear[6].

To further clarify the mechanism involving Opg as a crucial link between the bone and vascular systems, we have generated *Opg* knockout mice. Here we report that $Opg^{-/-}$ mice indeed develop a high-bone-turnover type osteoporosis. The aortic calcification in $Opg^{-/-}$ mice was observed. But serum calcium and phosphorus concentration remains normal, indicating that aortic calcification is not due to abnormal calcium and phosphorus metabolism.

1 Materials and methods

1.1 Materials

X-pPNT plasmid was provided by Dr. Pandolffi from Memorial Sloan-Kettering Cancer Center. PCR product cloning vector pGEM-Teasy was purchased from Promega Company. Cell culture medium and reagents were from Invitrogen and Chemicon. C57BL/6J and 129S1/Sv mouse strains were bred by Shanghai Research Center for Model Organisms. All molecular biology reagents were from Takara and NEB. Goat anti-OPG polyclonal antibody was from Santa Cruz. HRP labeled rabbit anti-goat antibody was from Sigma. PCR primers were synthesized by Shanghai San Gong Bio-technique LTD. The primer sequences are described as follows: *OPG5′* armU, 5′ CGTAGGATCCGTACCTCAGCCTCTGAAGAT 3′, *OPG5′* armD, 5′ TCGGTCTAGACAGGAGCTAGAAGAGACACA 3′; *OPG3′* armU, 5′ ACCGTCGACAGCCAGACAGCAGCTAAC 3′, *OPG3′* armD, 5′ GTGGCGGCCGCACAGCCAGGACTGTCAACA 3′; *OPG5′* JDU, 5′ ACCCACCATCTTCACTCACTTCTG 3′, *OPG5′* JDD, 5′ GCATCGCCTTCTATCGCCTTCTTG 3′; *OPG3′* JDU, 5′ GCTACCGGTGGATGTGGAAT 3′, *OPG3′* JDD, 5′ CAAATTCGTGCTCAGGTTAT 3′, *OPG*WT, 5′ GTAACGCCCTTCCTCACACTCACA 3′; *OPG*5PU, 5′ AAAAGGGCCAAAATCAAAATAATA 3′, *OPG*5PD, 5′ AGAGGGCAGAAGTGAGTGAAGATG 3′; *OPG*3PU, 5′ AGAGGGCAGAAGTGAGTGAAGATG 3′, *OPG*3PD, 5′ GGAAAACACCGGCCCTACTACATA 3′; *OPG*RTU, 5′ GTGGAAGGGCAAGAGCGTCGTG 3′, *OPG*RTD, 5′ CCAGAAGGGCCCGGAAGTAGTCA 3′.

1.2 Construction of gene targeting vector

The 5′ and 3′ homologous arms were amplified from ES cell genomic DNA by PCR using primer pairs of *OPG5′* armU, *Opg5′* armD and *Opg3′* armU, *Opg3′* armD, respectively. Targeting vector X-pPNT-*Opg* was constructed by inserting 5′ arm into *Bam*H Ⅰ and *Xba* Ⅰ site, and 3′ arm into *Sal* Ⅰ and *Not* Ⅰ site. The vector was confirmed by restriction endonuclease digestion and DNA sequencing.

1.3 Electroporation and screening of positive ES clone

The CJ7 ES cell line was maintained to passage 13 *in vitro*. Actively growing cells were trypsinized and resuspended in PBS buffer (with Ca^{2+}, Mg^{2+}) at a density of 1.2×10^7 cells/ml. Mix 0.8 ml of cell suspension with 30 μg of linearized targeting vector (digested with *Not* Ⅰ) in an electroporation cuvette (0.4 cm, Bio-Rad). For electroporation, cells were exposed to a single pulse at 240 V, 500 μF (Bio-Rad Gene Pulser Ⅱ), and replated to two 10 cm dishes containing a feeder layer. 24 hours after electroporation, drug selection was performed by adding 400 mg/L G418 and 2 μmol/L gancyclovir. Drug resistant colonies were picked after 7～8 day selection. Genomic DNA was isolated from ES cells in 48-well plate. Positive colonies were identified by PCR using primers: *Opg5′* JDU and *Opg5′* JDD, *Opg3′* JDU and *Opg3′* JDD, respectively. A 4.5 kb fragment from 5′ arm recombinant DNA and a 5 kb fragment from 3′ arm recombinant DNA should be observed. Southern blot was carried out by using ES cell genomic DNA digested with *Eco*R Ⅴ, and two probes of 586 bp fragment amplified by PCR using Opg5 and 3PU, and 815 bp fragment amplified by PCR using Opg5 and 3PD, respectively.

1.4 Production of chimeras

To generate chimeric mice, 15～20 recombinant ES cells were injected into C57BL/6J blastocysts, and then transferred into uterus of pseudopregnant mice. Pups were born and the degree of chimerism could be judged according to their coat-color combination.

1.5 Breeding of gene knockout mice

Male chimeras which chimeric rate is above 50% were mated with C57BL/6J female. Offspring derived from an ES cell-derived gamete would have grey hairs. After genotyping, mice heterozygous for *Opg* gene

knockout were intercrossed to generate homozygous mice and backcrossed to 129Sv background.

1.6 Genotyping of *Opg* knockout mice

Genotyping was identified by PCR with OpgWT, Opg5′ JDU and Opg5′ JDD primers in the same reaction system. 4.0 kb and 4.5 kb fragments could be separately amplified in $Opg^{+/+}$ (wild type) and $Opg^{-/-}$ mice (homozygous), both fragments in $Opg^{+/-}$ mice (heterozygous). Opg expression was detected by routine RT-PCR and Western blot.

1.7 Phenotype analysis for $Opg^{-/-}$ mice

The gross phenotypes, such as appearance, development, body weight, behavior, etc. were observed on a regular basis. Radiography was performed prior to the gross dissection on a soft X-ray system. Serum calcium, phosphorous and ALP activity were analyzed using automated equipment (Beckman, Fullerton, CA). Major organs were weighed and all tissues were fixed in formalin and embedded in paraffin, sectioned on a microtome, stained with hematoxylin, and counter-stained with eosin. Mineral density and bone mineral content were determined from left tibial metaphysis and tibial cortical shaft of mice using Mettler Toledo Balance (AG204, Swiss). All mice were injected with Tetracycline hydrochloride (Sigma-Aldrich Corp, 30 mg/kg body weight) 7 and 2 days prior to sacrifice for *in vivo* fluorescent labeling of mineralization sites. To evaluate bone quality, the mechanical characters of femora were measured by three-point bending test using the Instron Mechanical Testing Machine (Instron- 5543, USA).

2 Results

2.1 Generation of $Opg^{-/-}$ mice

Mouse *Opg* gene contains five exons encodes 401 amino acids including a signal peptide and seven structural domains. A targeting vector was constructed containing a 3.3 kb short arm and a 3.9 kb long arm of homologous fragments flanking a PGk-neo cassette. A

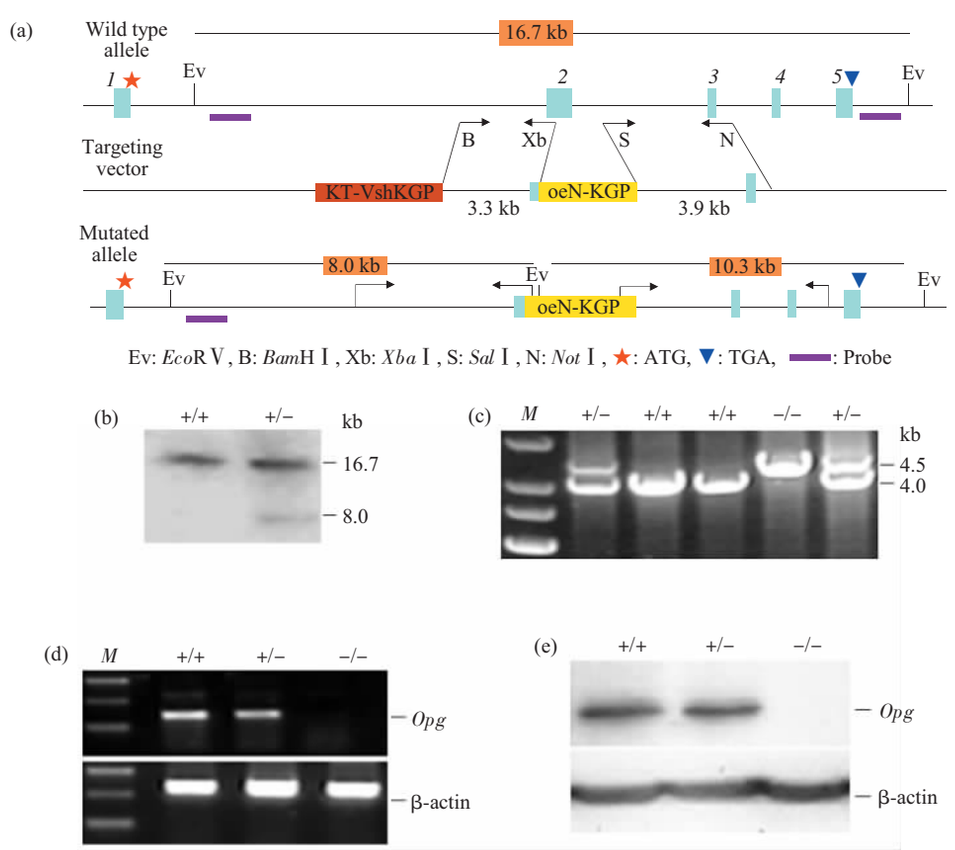

Fig. 1 *Opg* gene targeting strategy

(a) Schematic representation of gene targeting at the *Opg* locus. (b)Southern blot analysis by using ES cells genomic DNA digested with *Eco*R Ⅴ. +/+: Wild ES clone; +/−: Positive targeted clone. (c) Genotyping of *Opg* knockout mice by PCR. 4.0 kb and 4.5 kb fragments could be separately amplified in $Opg^{+/+}$ (wild type) and $Opg^{-/-}$ mice (homozygous mice), both fragments in $Opg^{+/-}$ mice (heterozygous mice). (d) RT-PCR and (e) Western blot analysis of RNA and protein from liver of wild-type (+/+), heterozygous (+/−), and homozygous (−/−) *Opg* knockout mice. The absence of Opg expression in $Opg^{-/-}$ mice was confirmed at both mRNA and protein levels.

409 bp region between exon 2 and intron 2 was replaced by PGk-neo cassette. The exon 2 encodes first two and part of third cysteine-rich domains. The strategy for targeted deletion of mouse *Opg* gene is outlined in Figure 1a. This strategy could effectively disrupt the coding region for the first two cysteine-rich domains of Opg that are required for its activity. Meanwhile, after homologous recombination it can also introduce a translation stop codon in-frame, preventing translation of any downstream *Opg* sequence. Chimeras generated from positive targeted clones transmitted the mutation through the germ line. Following heterozygous mating, homozygotes were identified and distinguished from heterozygotes and wild-type mice by PCR (Figure 1c). RT-PCR and Western blot analysis failed to detect Opg expression in $Opg^{-/-}$ mice (Figure 1d,e). $Opg^{-/-}$ mice had a normal morphological appearance and were viable and fertile.

2.2　*Opg*$^{-/-}$ mice exhibit osteoporosis and aortic calcification

Radiographic analysis of the skeleton of 2-month-old $Opg^{-/-}$ mice revealed a significant decrease in bone mass compared to wild-type littermates, and this low bone mass phenotype was observed in all mutant animals analyzed regardless of sex and at all stages analyzed (Figure 2a, b). Quantification of bone density in 2-month-old Opg-deficient mice and wild-type littermates was performed. The bone density in the $Opg^{-/-}$ mice at 2 month of age is (0.90 ±0.08) g/cm^3 versus (1.23 ±0.09) g/cm^3 in *wt* mice ($P < 0.01$). To evaluate bone quality, bone strength was measured on femurs by three-point bending test (Table 1). $Opg^{-/-}$ mice display a significant decrease in ultimate load, ultimate stress and Young's modulus compared with *wt* mice. Sections of thoracic aorta were stained with hematoxylin, and counter-stained with eosin. As shown in Figure 2c and 2d, normal arterial smooth muscle was stained as light pink in color, and calcified tissue was stained in dark blue. About 50% of 2- to 3-month-old $Opg^{-/-}$ mice exhibits medial vascular calcification in aorta.

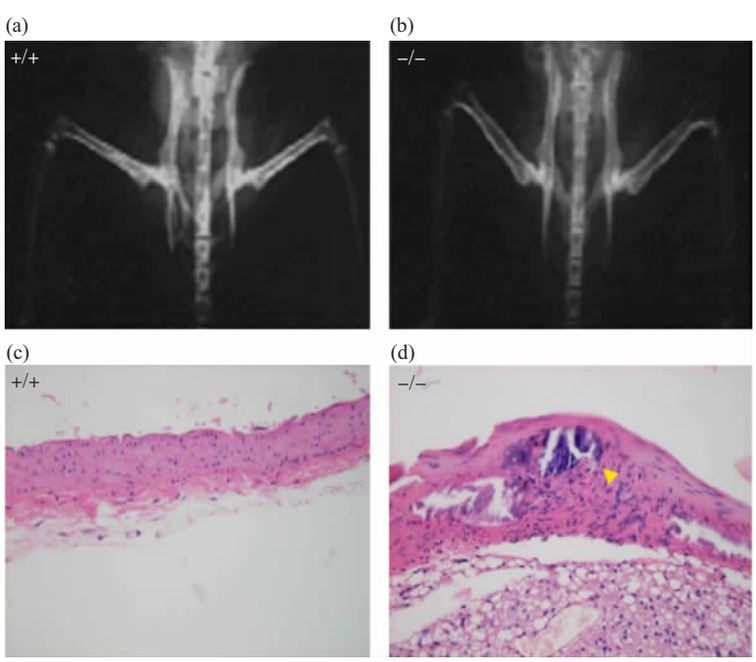

Fig. 2　*Opg*$^{-/-}$ mice exhibit osteoporosis and aortic calcification

(a, b) Radiographs of 2-month-old mice show decreased bone mineral density of leg, pelvis and vertebrae in $Opg^{-/-}$ mice compared with wild-type. (c, d) $Opg^{-/-}$ mice exhibite medial calcification (arrow) of aortic calcification (H&E stained, 40×).

Table 1　Bone mineral density and strength of *wt* and *Opg*$^{-/-}$ mice

Groups	BMD/(g·cm^{-3})	Ultimate load /N	Ultimate stress /MPa	Young's modulus/GPa
wt	1.23 ± 0.09	21.27 ± 7.45	122.50 ± 30.72	4.92 ± 1.89
$Opg^{-/-}$	0.90 ± 0.08[1)]	11.59 ± 4.38[1)]	62.16 ± 29.46[1)]	1.49 ± 0.83[1)]

[1)]Compared with *wt* mice, $P < 0.01$ ($n = 10$).

2.3 High bone turnover in Opg deficiency mice

Enzyme histochemistry was performed to determine the level of tartrate-resistant acid phosphatase activity (TRAP), that can specifically stains osteoclasts red. The number of osteoclasts is sharply increased in the trabecular bone of 2-month-old $Opg^{-/-}$ mice ((3.50±0.35)/mm *vs*. (0.79±0.10)/mm, $P<0.01$). The same result was also observed in cortical bone (Figure 3b). The increased osteoclasts may lead to enhanced bone resorption which results in significant loss of bone mass. Osteoblasts along the bones of $Opg^{-/-}$ mice were more cuboidal than those in *wt* mice. The number of cuboidal osteoblasts per millimeter of trabecular bone perimeter in 2-month-old $Opg^{-/-}$ mice is increased about threefold ((14.66 ± 0.99)/mm *vs*. (5.53 ±0.41)/mm, $P<0.01$). The bone mineral accumulation rate in $Opg^{-/-}$ mice is also significantly increased compared with those in $Opg^{-/-}$ mice ((42.50 ±10.08) μm / day vs. (21.67 ± 4.92) μm / day, $P < 0.01$). Consistent with this finding, an increase of osteoblast activity evidenced by morphological change of osteoclasts, elevated serum alkaline phosphatase activity (which can be a marker of osteoblast activity) was also observed in mutant mice. At 2 month of age, $Opg^{-/-}$ mice have significantly elevated serum alkaline phosphatase activity compared to *wt* mice ((418±23.07) U/L vs. (114±9.12) U/L, $P<0.01$) (Table 2).

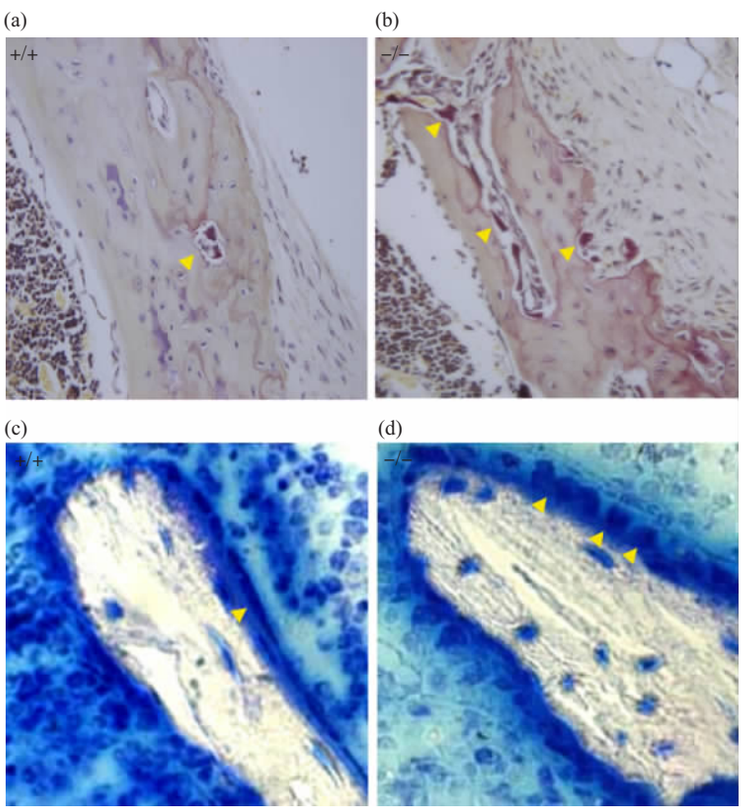

Fig. 3 High bone turnover in $Opg^{-/-}$ mice

(a, b) TRAP staining of femoral cortical shaft of *wt* and $Opg^{-/-}$ mice. Yellow arrowheads indicate TRAP positive osteoclasts. (c, d) Arrows indicate osteoblasts along the bone surface (H&E stained,40 ×). Osteoblasts of $Opg^{-/-}$ mice appear more cuboidal in shape than those of *wt* mice.

Table 2 Bone turnover in *wt* and $Opg^{-/-}$ mice

Groups	OC/(Numbers/mm)	OB/(Numbers /mm)	MAR /(μm/day)	ALP/(U/L)
wt	0.79 ± 0.10	5.53 ± 0.41	21.67 ± 4.92	114 ± 9.12
$Opg^{-/-}$	3.50 ± 0.35[1)]	14.66 ± 0.99[1)]	42.50 ± 10.08[1)]	418 ± 23.07[1)]

[1)] Compared with *wt* mice, $P < 0.01$ ($n = 10$).

2.4 Calcium and phosphorus metabolism in *Opg*$^{-/-}$ mice

The contents of calcium and phosphorus in *Opg*$^{-/-}$ tibias were (11.74 ±0.38) mg and (1.07 ±0.21) mg, respectively, compared to (12.32 ± 0.22) mg and (1.53 ± 0.34) mg in *wt* tibias ($P < 0.01$). But there were no significant differences in serum concentrations of calcium and phosphorus between *wt* and *Opg*$^{-/-}$ mice. Our results show that calcium and phosphorus that released from bone were not accumulated in peripheral blood.

Table 3 Parameters of calcium and phosphorus metabolism in *Opg*$^{-/-}$ mice

Groups	Bone calcium/mg	Bone phosphorus/mg	Serum calcium/(nmol·L^{-1})	Serum phosphorus/(nmol·L^{-1})
wt	12.32 ± 0.22	1.53 ± 0.34	2.52 ± 1.10	2.55 ± 0.38
Opg$^{-/-}$	11.74 ± 0.38[1)]	1.07 ± 0.21[1)]	2.45 ± 0.05	2.99 ± 0.55

[1)] Compared with *wt* mice, $P < 0.01$ (n=10).

3 Discussion

OPG is expressed both in bone and vasculature as reported by Bucay *et al*[4]. We have observed severe osteoporosis and vascular calcification in *Opg* knockout mice. In bone system, RANKL is an essential cytokine for the formation and activation of osteoclasts and promotes bone resorption. This effect could be antagonized by OPG as its endogenous counterpart. But the exact role of OPG in normal or pathological vascular biology remains unclear. Our results show that the serum level of calcium and phosphorus was not different between *Opg*$^{-/-}$ and *wt* mice [7]. In rat model, *Opg* treatment prevents warfarin-induced vascular calcification with normal concentrations of calcium and phosphorus [8]. Those results imply that arterial calcification observed in *Opg*-deficient mice is not associated with calcium/phosphate homeostasis.

Vascular calcification, long thought to result from passive degeneration, involves a complex, regulated process of biomineralization resembling osteogenesis. Evidence indicates that proteins controlling bone mineralization are also involved in the regulation of vascular calcification[9]. We found increases both in the number of cuboidal osteoblasts alone bone surface and in bone formation rate in *Opg* deficiency mice. Due to exhibiting osteoporosis in the mice, the active bone formation was commonly explained by reflecting the coupling between osteoclast-mediated resorption and osteoblast-mediated bone synthesis. The enhancement of bone mineralization function in *Opg*$^{-/-}$ mice was ignored. The aortic calcification in *Opg*$^{-/-}$ mice occurs in the media arterial wall where arterial vascular smooth muscular cells (AVSMCs) exist. *Opg*, Rankl and Rank molecules are all expressed in the cells which can be transformed to osteoblast-like cells and have mineralization function under certain conditions [10]. So we postulated that OPG/RANKL is important in vascular calcification through direct effects on AVSMCs. Unbalance of OPG/RANKL might results in arterial calcification by AVSMCs phenotypic transition. To date, there are no reports regarding potential biological effects of OPG on AVSMCs calcification [11], and such insights therefore await further research.

It was reported that OPG gene homologous deletion leads to Paget's disease and increase arterial calcification in Paget's disease[12, 13]. *Opg* deficient mice exhibited bone loss with an increase in both bone resorption and formation, which just like high bone turnover postmenopausal osteoporosis. In fact, bone mineral density in postmenopausal women significantly decreases with the progression of aortic calcification [14]. In conclusion，*Opg* knockout mice model is a suitable tool to further study the relation of osteoporosis and vascular calcification. It will be helpful for developing new therapeutic strategies for bone and vascular system.

References

1 Tolar J, Teitelbaum S L, Orchard P J. Osteopetrosis. N Engl J Med, 2004, **351**: 2839～2849

2 Doherty T M, Fitzpatrick L A, Inoue D, *et al*. Molecular, endocrine, and genetic mechanisms of arterial calcification. Endocr Rev, 2004, **25**: 629～672

3 Schulz E, Arfai K, Liu X, *et al*. Aortic calcification and the risk of osteoporosis and fractures. J Clin Endocrinol Metab, 2004, **89**: 4246～4253

4 Bucay N, Sarosi I, Dunstan C R, *et al*. Osteoprotegerin-deficient

mice develop early onset osteoporosis and arterial calcification. Genes Dev, 1998, **12**: 1260～1268

5 Min H, Morony S, Sarosi I, *et al*. Osteoprotegerin reverses osteoporosis by inhibiting endosteal osteoclasts and prevents vascular calcification by blocking a process resembing osteoclastogenesis. J Exp Med, 2000, **192**: 463～474

6 Hofbauer L C, Schoppet M. Clinical implications of the osteoprotegerin/RANKL/RANK system for bone and vascular disease. JAMA, 2004, **292**: 490～495

7 Nakamura, Udagawa N, Matsuura S, *et al*. Osteoprotegerin regulates bone formation through a coupling mechanism with bone resorption. Endocr, 2003, **144**: 5441～5449

8 Price P A, June H H, Buckley J R, *et al*. Osteoprotegerin inhibits artery calcification induced by warfarin and by vitamin D. Arterioscler Thromb Vasc Biol, 2001, **21**: 1610～1616

9 Vattikuti R, Towler D A. Osteogenic regulation of vascular calcification: an early perspective. Am J Hysiol Endocrinol Metab, 2004, **286**: 686～696

10 Steitz S A, Speer M Y, Curinga G, *et al*. Smooth muscle cell phenotypic transition associated with calcification: upregulation of cbfa1 and downregulation of smooth muscle lineage markers. Circ Res, 2001, **89**: 1147～1154

11 Collin-Osdoby P. Regulation of vascular calcification by osteoclast regulatory factors RANKL and osteoprotegerin. Circ Res, 2004, **95**: 1046～1057

12 Hofbauer L C, Schoppet M. Osteoprotegerin deficiency and juvenile Paget's disease. N Engl J Med, 2002, **347**: 1622～1623

13 Laroche M, Delmotte A. Increased arterial calcification in Paget's disease of bone. Calcif Tissue Int, 2005, **77**: 129～133

14 Hak A, Pols H, van Hemert A, *et al*. Progression of aortic calcification is associated with metacarpal bone loss during menopause: a population-based longitudinal study. Arterioscler Thromb Vasc Biol, 2000, **20**: 1926～1931

骨保护素 (*Opg*) 基因敲除小鼠发生高转换型骨质疏松和动脉钙化 *

许 勇[1,2] 杨 桦[2] 乔建珏[1,2] 李西华[1,4] 严兰珍[2]
王 龙[2,3] 徐国江[2] 费 俭[2] 傅继梁[2] 王铸钢[1,2,3,4]**

([1]上海交通大学医学院遗传学教研室，上海 200025；[2]上海南方模式生物研究中心，上海 201203；
[3]上海交通大学附属瑞金医院医学遗传学国家重点实验室，上海 200025；
[4]中国科学院上海生命科学研究院和上海交通大学医学院健康科学研究所基因工程实验室，上海 200025)

摘要 骨质疏松以及动脉钙化均是危害极大的临床常见病变，骨保护素 (OPG) 可能是联系两者的分子之一. 构建替换型载体 pXpPNT-OPG，利用同源重组，将编码前 3 个蛋白质结构域的小鼠 *Opg* 基因组第二外显子序列剔除掉. 通过胚胎干细胞 (ES) 基因打靶获得了正确重组的 ES 细胞克隆，ES 细胞显微注射后获得嵌合体小鼠，交配传代获得杂合子和纯合子小鼠. RT-PCR 和蛋白质印迹实验结果显示，纯合子小鼠没有 *Opg* 基因的表达. 纯合子小鼠骨量丢失明显，骨生物力学指标明显下降，发生严重的骨质疏松，此外，还有 50%以上的纯合子小鼠在早期出现动脉中层钙化. 小鼠破骨功能亢进，与此同时，成熟成骨细胞数量增加，矿化功能强于野生型. *Opg* 基因缺失小鼠骨中钙和磷大量流失，而血清中水平没有变化，这提示钙磷代谢异常不是 OPG 缺失导致动脉钙化的原因. 对建立的 *Opg* 基因敲除小鼠模型进一步深入的研究，将有助于说明动脉钙化和骨质疏松症相互联系的分子机制，为防治骨质疏松症和动脉钙化的并发提供理论基础支持.

关键词 骨保护素 (*Opg*) 基因敲除小鼠，骨质疏松，动脉钙化，骨转换，钙磷代谢
学科分类号 Q78

*国家高技术研究发展计划项目(2001AA216081, 2004AA216081), 国家自然基金杰出青年科学家基金(39925023), 国家教育部基金项目(00TPJS111), 上海市科技发展基金项目(99JC14029, 99XD14005), 上海市教育局 E- 研究院(E03003)资助.
** 通讯联系人. Tel/Fax: 021-64457997, E-mail: zhugangw@shsmu.edu.cn
收稿日期：2006-08-11，接受日期：2006-12-13